NeuroImage: Clinical 44 (2024) 103699

Contents lists available at ScienceDirect

NeuroImage: Clinical

journal homepage: www.elsevier.com/locate/ynicl

Tau-network mapping of domain-specific cognitive impairment in Alzheimer's disease

Ying Luan [a,b], Anna Rubinski [b], Davina Biel [b], Diana Otero Svaldi [c], Ixavier Alonzo Higgins [c], Sergey Shcherbinin [c], Michael Pontecorvo [c], Nicolai Franzmeier [b,d], Michael Ewers [b,e,*], for the Alzheimer's Disease Neuroimaging Initiative ADNI[1]

[a] Department of Radiology, Zhongda Hospital, School of Medicine, Southeast University, Nanjing, China
[b] Institute for Stroke and Dementia Research (ISD), University Hospital, Ludwig Maximilian University (LMU), Munich, Germany
[c] Eli Lilly and Company, Indianapolis, IN, USA
[d] Munich Cluster for Systems Neurology (SyNergy), Munich, Germany
[e] German Center for Neurodegenerative Diseases (DZNE), Munich, Germany

ARTICLE INFO

Keywords:
tau-PET
Functional connectivity
Symptom-lesion mapping
Alzheimer's disease
Cognitive domain

ABSTRACT

Fibrillar tau gradually progresses in the brain during the course of Alzheimer's disease (AD). However, the contribution of tau accumulation in a given brain region to decline in different cognitive domains and thus phenotypic heterogeneity in AD remains unclear. Here, we leveraged the functional connectome to link the locality of tau accumulation to domain-specific cognitive impairment.

In the current study, we mapped regional tau-PET accumulation onto the normative functional connectome. Subsequently, we cross-validated in two samples of AD-patients the associations between the tau-connectivity profiles and cognitive domains (episodic memory, executive function, or language). Lastly, we tested the effect of local tau-PET accumulation on the domain-specific tau-lesion networks and cognition.

We identified cognitive-domain-specific tau-lesion networks, where closer topological proximity of tau-PET locations to a network was predictive of worse impairment in that domain. Higher tau-PET was associated with decreased domain-specific network connectivity, and the decrease in connectivity was associated with lower domain-specific cognition.

The tau locations' connectivity profile explained domain-specific cognitive impairment, where disrupted connectivity may underlie the effect of tau on cognitive impairment.

1. Introduction

Alzheimer's disease (AD) is characterized by progressive cognitive decline and accounts for the majority of age-related dementia cases (Alzheimer's Association, 2020). Beta-amyloid (Aβ) plaques and neurofibrillary tangles (NFTs) are the disease-defining pathologies, but it is fibrillar tau that is the stronger predictor of cognitive decline in AD (La Joie et al., 2020; Nelson et al., 2012). Unlike amyloid plaques which are more globally distributed in the brain, fibrillar tau occurs in spatially circumscribed brain areas in mild stages of the disease. Tau pathology typically spreads from the medial temporal lobe and connected brain regions in the posterior parietal and medial frontal lobe (Braak and Braak, 1991; Braak and Del Tredici, 2018), but the spatial distribution is not uniform and substantially differs between individuals as suggested by neuroimaging studies on fibrillar tau in AD (Mohanty et al., 2023; Murray et al., 2011; Vogel et al., 2023). The spatial heterogeneity of tau deposition may be a significant source of symptomatic variability in AD (Bejanin et al., 2017; Devous et al., 2021; Digma et al., 2019). Cognitive abilities emerge from the interaction of multiple brain areas within functional network rather than isolated anatomical areas. Therefore, a challenge is to match the anatomical location of tau pathology to deficits in diverse cognitive domains.

* Corresponding author at: Institute for Stroke and Dementia Research, Klinikum der Universität München, Feodor-Lynenstr. 17, 81377 Munich, Germany.
E-mail address: michael.ewers@med.uni-muenchen.de (M. Ewers).

[1] Data used in preparation of this article were obtained from the Alzheimer's Disease Neuroimaging Initiative (ADNI) database (adni.loni.usc.edu). As such, the investigators within the ADNI contributed to the design and implementation of ADNI and/or provided data but did not participate in analysis or writing of this report. A complete listing of ADNI investigators can be found in the appendix ("ADNI_coinvestigators.docx").

https://doi.org/10.1016/j.nicl.2024.103699
Received 15 April 2024; Received in revised form 1 October 2024; Accepted 28 October 2024
Available online 30 October 2024

Recently, symptom-network mapping approaches have been developed which elegantly translates an anatomical location of a brain alteration to its topographic location at the network level in order to understand its impact on a particular cognitive or behavior function (Boes et al., 2015; Fox, 2018). Findings from lesion-network mapping studies in psychiatric and neurodegenerative diseases demonstrated that the closer a brain lesion (e.g. atrophy) was connected to core brain regions underlying a cognitive ability, the stronger was the cognitive impairment (Tetreault et al., 2020). Such a network perspective unlocks the predictive power of brain location for understanding the emergence of cognitive/behavioral phenotypes.

Here, we leveraged the symptom-network mapping approach in order to first develop a clinico-topographical map of local tau deposition for the explanation of decline in specific cognitive domains including episodic memory, executive function, and language. In a first step, we located tau deposition within the normal functional connectome and identified those functional networks that contributed to explaining impairment in major cognitive domains. Next, we tested whether disruption of functional connectivity in the identified domain-specific networks explains the association between regional tau-PET accumulation and domain-specific cognitive impairment. We hypothesized that closer topographic proximity of local tau-PET deposition to a domain-specific functional network is predictive of stronger impairment in the associated cognitive domain. Furthermore, we hypothesized that the reduced patient-level functional connectivity between the tau-lesion locations and a cognitive-domain network underlies stronger impairment in that cognitive domain.

2. Methods

2.1. Participants

2.1.1. Alzheimer's disease neuroimaging Initiative (ADNI)

We included 234 cognitively normal (CN) controls exhibiting no abnormal global amyloid-PET binding (CN-Aβ-) and 218 participants with abnormal global amyloid-PET binding (Aβ +), including 73 CN-Aβ+, 88 participants with mild cognitive impairment (MCI-Aβ +) and 57 AD dementia patients from ADNI (recruitment wave 3). ADNI is an observational multicenter study on the investigation of biomarker and cognitive changes in Alzheimer's disease (Weiner et al., 2017), where the data are freely available to researchers (https://adni.loni.usc.edu/). The clinical diagnostic criteria in ADNI were described previously (Petersen et al., 2010). The Aβ status (Aβ-/+) was quantitatively determined according to pre-established cutoff values for abnormal global amyloid PET accumulation (Aβ+, florbetapir PET SUVR > 1.11 or global florbetaben PET SUVR > 1.08, for details see https://tinyurl.com/3jjn7mu7 and https://tinyurl.com/5yfe9rny). Ethical approval and written informed consent from all participants were obtained prior to the study by ADNI investigators.

2.1.2. The Avid 18F-AV1451-A05 study ("A05")

We included a total of 116 elderly participants (> 50 yrs) from an observational clinical trial "18F-AV1451-A05" (Pontecorvo et al., 2019; Pontecorvo et al., 2017), (henceforth referred to "A05"; for the inclusion and exclusion criteria see https://clinicaltrials.gov/ct2/show/NCT02016560). The sample was comprised of 49 CN Aβ- subjects, 4 CN Aβ+, 33 MCI Aβ + and 24 Aβ + AD dementia patients (for the clinical diagnostic criteria see (Pontecorvo et al., 2017). The Aβ status was determined based on visual rating of florbetapir amyloid PET images by two experienced readers (Pontecorvo et al., 2019; Pontecorvo et al., 2017). The study was approved by the centers' institutional review boards. All subjects or their authorized representatives provided signed informed consent. The study was conducted in accordance with the Declaration of Helsinki and the International Conference on Harmonization (ICH) Good Clinical Practice (GCP) guideline.

2.2. Neuropsychological assessment

In ADNI, we employed composite scores of episodic memory (i.e. ADNI-MEM), executive function (i.e. ADNI-EF) and language (i.e.ADNI-LAN) centrally computed by the ADNI neuropsychology core team as previously described https://adni.bitbucket.io/reference/docs/UWNPSYCHSUM/adni_uwnpsychsum_doc_20200326.pdf.

In A05, we computed composite scores for executive function (i.e. A05-EF) and language domains (i.e. A05-LAN), while using only a single score for episodic memory (A05-MEM). For the A05-EF score, we included category fluency-animals and digit span backwards, digit symbol substitution test, trail making test A & B, and clock drawing. For the A05-LAN score, we included category fluency-animals and Boston naming test. For episodic memory (A05-MEM), we used the Logical memory immediate recall score only, as the test of delayed recall showed floor effects in the sample, with 14 out of 61 Aβ + subjects scoring zero. The composite cognitive scores of A05-EF and A05-LAN were computed according to a previously established method (Langbaum et al., 2014). Specifically, the scores for each test were standardized to range between 0 and 1 by subtracting the minimum possible score for this test from each original score divided by the range (i.e. difference of the maximum and minimum possible scores). For the tests without an established maximum possible score (e.g., Category fluency test), a maximum possible score was defined as 2 standard deviations over the score averaged across subjects (Malek-Ahmadi et al., 2018). The composite scores for each domain were calculated as the mean of the standardized values across the tests of a particular cognitive domain. Each cognitive score was corrected for age, gender, education years and diagnosis in linear regression

2.3. Structural and functional MRI acquisition and preprocessing

In ADNI, three-dimensional (3D) T1-weighted images were acquired on 3 T scanners according to a standardized protocol with 1-mm isotropic voxel size (TR = 2300 ms). Parameter details can be found on http://adni.loni.usc.edu/wp-content/uploads/2017/07/ADNI3-MRI-protocols.pdf. In order to derive spatial normalization parameters, T1-weighted images were spatially registered to Montreal Neurological Institute (MNI) template using high-dimensional transformation via Advanced Normalization Tools (ANTs) (Avants et al., 2011). In A05, structural 3D T1 weighted MRI images were acquired as well. The parameters for the spatial normalization of flortaucipir PET images (see below) were estimated based on high-dimensional registration as described previously (Pontecorvo et al., 2017).

In addition to structural MRI, resting-state fMRI data were recorded in ADNI, using a 3D echo planar imaging sequence with 3.4-mm isotropic voxel size and TR = 3000 ms (197–200 volumes). The resting-state fMRI data preprocessing included alignment, co-registration to the native-space T1 images, spatial smoothing using an 8 mm full-width at half maximum gaussian kernel, motion correction by Independent Component Analysis-based Automatic Removal Of Motion Artifacts (ICA-AROMA), detrending, band-pass filtering (0.01–0.08 Hz), nuisance regression (i.e., 6 motion parameters, mean signal extracted from cerebrospinal fluid and white matter masks), and normalization to MNI standard space using the T1-image derived transformation parameters.

2.4. Acquisition and processing of tau-PET

In ADNI, flortaucipir PET was recorded 75–105 min (six 5-min time blocks) after injection of the flortaucipir F18 tracer. The PET images were realigned and averaged into a single image for each subject (Jagust et al., 2015) (also see ***http://adni***.loni.usc.edu/methods/pet-analysis-method/pet-analysis/#pet-pre-processing-container). In A05, flortaucipir PET images were acquired 80–100 min after tracer injection (in four 5-min. frames) and averaged into subject level single images. The

processing of the flortaucipir PET scans from ADNI and A05 is detailed in the Supplementary section 1.1. Briefly, the flortaupicir PET scans were spatially normalized using the T1 MRI derived spatial transformation parameters, and intensity normalized using inferior cerebellar gray as reference ROI to compute standardized uptake value ratios (SUVR). ROI-level flortaucipir PET values were subsequently extracted based on the 400 cortical-ROI-Schäfer atlas (Schaefer et al., 2018).

2.5. Computation of ROI W-scores for tau-PET scans

A flow chart of the subsequently applied data analysis pipeline is provided in Fig. 1. In order to identify regions of abnormally increased tau-PET (referred to as tau-lesion), we computed W-scores of tau-PET ROI in the Aβ + subjects, adopting a modified procedure to compute neuroimaging-based W-scores (Ossenkoppele et al., 2015; Tetreault et al., 2020) (Fig. 1A, see for details see Supplementary Section 1.2). A subject's tau-PET W-score reflects the standardized deviation of a ROI tau-PET SUVR value in an Aβ + subject from the group average ROI tau-PET SUVR in the Aβ- group. We defined a tau-PET lesion as a ROI tau-PET W-score > 2, similar to a previous approach on W-score based lesion identification of brain atrophy in AD (Tetreault et al., 2020). For each subject, the global tau-PET W-scores were calculated by averaging the W-scores across all the ROIs.

2.6. Tau-lesion network mapping

We adopted a recently developed "lesion network mapping" method (Darby et al., 2017) to identify those brain regions that were functionally connected to the single-subject tau lesions in ADNI and A05 datasets (Fig. 1B). To this end, we superimposed each tau-PET lesion ROI onto 1000 spatially normalized (i.e., to MNI space) resting-state fMRI data from the Human Connectome Project (HCP, http://www.humanconnectomeproject.org/) (Smith et al., 2013) to generate the functional-connectivity maps for each tau-PET lesions site by seed-based functional connectivity analyses. In seed-based analysis, the Pearson-Moment correlations between the fMRI BOLD time series of a given tau-PET lesion and each of the 400 ROIs were computed within each of the 1000 rsfMRI scans from HCP. The resulting Pearson *r*-scores maps of each tau-PET lesion (tau-lesion-network maps) were subsequently Fisher-z transformed and subjected to one-sample t-tests, thus yielding unthresholded t-maps of connectivity of each tau-PET lesion (i.e. the tau-lesion network maps).

2.7. Cognitive domain-specific tau-lesion network mapping

Having mapped the tau-lesion networks, we next determined which connections of the tau-PET lesions are associated with worse performance in a particular cognitive domain including episodic memory, executive function, and language (Fig. 1C). To this end, we applied a partial least squares regression (PLSR) analysis in our training sample (ADNI). PLSR is a regression method that reduces a larger number of correlated predictors to latent variables, and is suitable to deal with potential multicollinearity among predictors (Krishnan et al., 2011). We conducted for each cognitive domain a PLSR analysis, including the tau-lesion-network t-map values described above as the independent variables and the adjusted domain-specific cognitive composite scores as the dependent variable. This yielded three cognitive-domain specific tau-lesion-network maps which indicated the strength of the association between tau-lesion connections and performance in a particular cognitive domain (for details see Supplementary Section 1.3).

2.8. Subject-level functional connectivity assessment

Subject-level functional connectivity was assessed based on rsfMRI available in 241 Aβ + from ADNI. We applied high-dimensional group independent-component-analysis (ICA) (Beckmann and Smith, 2004) to the preprocessed fMRI data. We chose n = 100 ICs to be estimated in order to render the ICA comparable to that used for the generation of an IC template (Miller et al., 2016) used as the reference ICs here. Out of 100 ICs estimated, a total of 54 ICs were deemed non-artifactual by spatial matching with the previously established ICs template from the UKBiobank (Miller et al., 2016). The thresholded IC maps (z > 5) were used as nodes in subsequent connectivity analyses (for details see Supplementary Section 1.4). We subsequently spatially matched the ICA-derived nodes against the tau-PET lesion locations and the ROIs of the domain-specific tau-lesion networks, and computed the subject-level functional connectivity between the IC time-series of these tau-PET and functional network nodes for each of the three domain-specific tau-lesion networks. This resulted for each subject in a connectivity matrix of correlations between tau-lesion ROIs and network ROIs for each cognitive-domain specific network. All positive correlations were averaged to generate subject-level tau-ROI functional connectivity scores for each cognitive-domain network.

2.9. Statistics

First, we tested our main hypothesis that stronger connectivity between the tau-PET lesion locations and the domain-specific tau-lesion network is associated with lower performance in the respective cognitive domain. To this end, we tested in separate linear regression analyses for each cognitive domain, whether the average functional connectivity from tau-PET lesion locations to the ROIs of a domain-specific tau-lesion network is associated with lower cognitive performance in that domain, controlled for age, gender, years of education and diagnosis. In order to test for the specificity of predictive performance of each domain-specific tau-lesion network, we applied linear regression models for each domain-specific network and the cognitive scores of each domain, additionally controlling for the performance in the other cognitive domains.

Next, we tested the hypothesis that tau-PET levels in a tau-lesion location are associated with reduced patient-level functional connectivity in the Aβ + group. To this end, we tested in linear regression analyses the tau-PET W-score averaged across lesion locations as a predictor of the average functional connectivity between the tau-lesion locations and a cognitive domain-specific tau-lesion network, controlled for age, gender, years of education, diagnosis, and MRI scanner manufacturer (resulting in 3 regression analysis, one for each cognitive domain specific network). In order to test functional connectivity alterations as a predictor of cognitive impairment, we employed a linear regression analysis including this time the tau-lesion- network connectivity as a predictor of cognitive performance in a given domain, resulting in another 3 different regression analyses. We employed mediation analysis to test whether alteration of functional connectivity to domain-specific tau-lesion networks mediates the effect of tau-PET W-scores on cognitive performances in the corresponding domain. All mediation models were controlled for age, gender, years of education, diagnosis, and MRI scanner manufacturer. The statistical significance of the mediation model was determined based on the 95 % confidence interval (95 % CI) of the average causal mediation effect, using bootstrapping with 1000 iterations. All regression analysis were controlled for the effects of age, gender, education years, diagnosis, and MRI scanner manufacturer. In bootstrapped regression analyses, the partial R^2 (adjusted for covariates) was compared between connectivity-weighted and alternate predictors. We accounted for multiple testing to guard against Type I error accumulation, using a Bonferroni corrected significance threshold. All analyses were performed using the R statistical software package (r-project.org).

3. Results

Basic characteristics of the participants split by diagnostic subgroups are shown for the ADNI and A05 studies in Table 1. Overall, the Aβ +

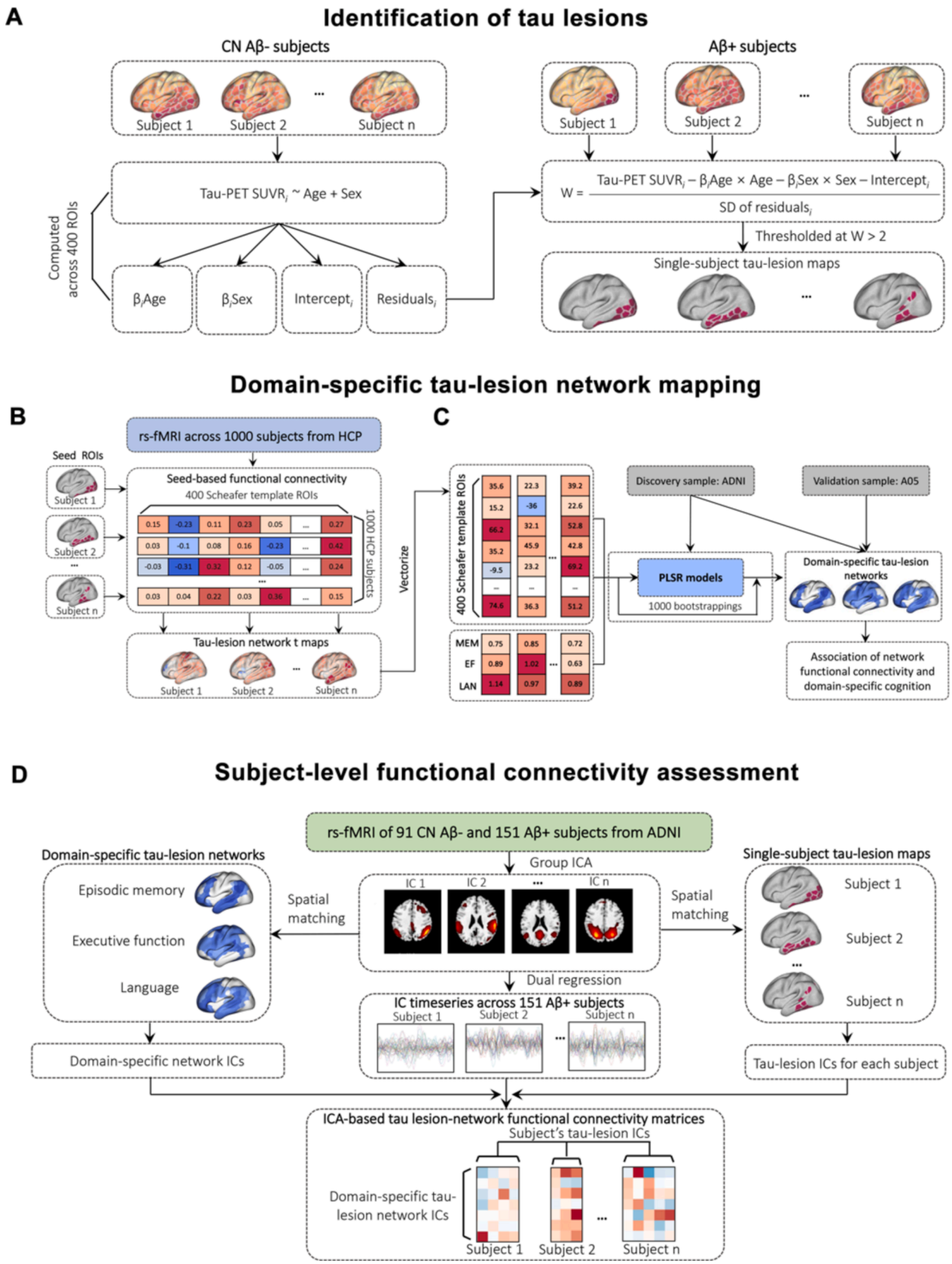

(caption on next page)

Fig. 1. Schema of the data analysis pipeline. (A) Subject-level W-scores of tau-PET SUVRs were computed for each ROI in the Aβ+ participants as the standardized deviation of tau-PET ROI SUVRs from the Aβ- CN group, adjusted for the influence of age and sex. Tau lesions were defined as tau-PET ROI W-scores > 2. (B) Single-subject tau-PET lesion ROIs were superimposed onto the 1000 rsfMRI scans from the HCP, and functional connectivity was computed between each tau-lesion ROIs and the remaining ROIs across the 1000 HCP subjects. ROI-wise one-sample *t*-test was conducted to generate tau-lesion network t-maps for each of the subjects. (C) PLSR was applied to estimate the association between domain-specific cognitive performances and tau-PET lesion network t-maps for each of the 3 cognitive domains in ADNI. Statistical significance of the PLRS-derived regression coefficients was determined by 1000 bootstrapped iterations for each of the cognitive domains, resulting in domain-specific tau-PET lesion network map. The association of averaged functional connectivity to each tau-lesion network and domain-specific cognitive performance was tested in ADNI discovery sample and A05 validation sample. (D) ICA was applied to resting-state fMRI scans obtained in a subset of patients in ADNI. ICs were spatially matched to the tau-PET lesion ROIs on the one hand and the ROIs in each of the domain-specific tau-lesion networks – which had been determined in steps B & C – on the other hand. The connectivity between IC times series of tau-PET lesions ROIs and domain-specific network ROIs were computed which were used in subsequent statistical analyses (see Statistics section).

Table 1
Sample characteristics.

ADNI	**CN Aβ- (n = 234)**	**CN Aβ+ (n = 73)**	**MCI Aβ+ (n = 88)**	**AD Dementia (n = 57)**	**p-value**
Age	71.50 (6.58) [b,c,d]	74.55 (7.38) [a]	74.54 (7.34) [a]	76.45 (8.91) [a]	<0.001
Gender (f/m)	144/90	44/29	41/47	27/30	0.040
Years of education	16.82 (2.33) [d]	16.66 (2.44) [d]	16.13 (2.55)	15.49 (2.44) [a,b]	0.001
ADAS11	8.40 (2.62) [c,d]	9.44 (3.45) [c,d]	12.84 (4.17) [a,b,d]	22.69 (6.70) [a,b,c]	<0.001
MMSE	29.15 (1.08) [c,d]	28.85 (1.46) [d,c]	27.41 (2.24) [a,c,d]	21.96 (3.84) [a,b,c]	<0.001
ADNI-MEM	1.05 (0.58) [b,c,d]	0.84 (0.57) [a,c,d]	0.12 (0.61) [a,b,d]	−0.77 (0.62) [a,b,c]	<0.001
ADNI-EF	1.22 (0.78) [b,c,d]	0.86 (0.83) [a,c,d]	0.24 (0.92) [a,b,d]	−0.88 (1.16) [a,b,c]	<0.001
ADNI-LAN	0.94 (0.72) [c,d]	0.75 (0.74) [c,d]	0.25 (0.87) [a,b,d]	−0.64 (1.02) [a,b,c]	<0.001
A05	**CN Aβ- (n = 49)**	**CN Aβ+ (n = 4)**	**MCI Aβ+ (n = 33)**	**AD Dementia (n = 24)**	**p-value**
Age	67.76 (10.36) [d]	77.75 (8.10)	71.91 (8.44)	76.04 (9.54) [a]	0.003
Gender (f/m)	22/27	2/2	15/18	14/10	0.727
Years of education	15.57 (1.94)	15.00 (2.58)	16.21 (3.08)	14.92 (2.89)	0.288
ADAS11	5.63 (3.44) [c,d]	6.00 (2.93) [d]	11.45 (4.41) [a,d]	21.75 (7.05) [a,b,c]	<0.001
MMESE	29.49 (0.51) [c,d]	29.75 (0.50) [d]	27.12 (1.96) [a,d]	21.46 (4.01) [a,b,c]	<0.001
Logical memory immediate recall	13.73 (4.52) [c,d]	13.75 (5.32) [c,d]	7.91 (3.19) [a,b,d]	4.33 (3.20) [a,b,c]	<0.001
A05-EF	0.72 (0.08) [c,d]	0.70 (0.11) [d]	0.59 (0.10) [a,d]	0.43 (0.17) [a,b,c]	<0.001
A05-LAN	0.81 (0.11) [c,d]	0.74 (0.09) [d]	0.68 (0.10) [a,d]	0.50 (0.16) [a,b,c]	<0.001

Values are displayed as mean (standard deviation).
p-values were derived from ANOVA for continuous measures and from Chi-squared tests for categorical measures.
[a] significantly different from CN-Aβ−; [b] significantly different from CN-Aβ+; [c] significantly different from MCI-Aβ+; [d] significantly different from AD dementia via post hoc Tukey test.
Abbreviations: CN = cognitively normal; MCI = mild cognitive impairment; AD = Alzheimer's disease; Aβ = amyloid β; m = male; f = female; ADAS = Alzheimer's Disease Assessment Scale–Cognitive subscale; MMSE = Mini-Mental State Exam; CL = Centiloid; ADNI-MEM = memory composite score for ADNI sample; ADNI-EF = executive function composite score for ADNI sample; ADNI-LAN = language composite score for ADNI sample; SUVR = standardized uptake value ratio; A05-MEM = memory composite score for A05 sample; A05-EF = executive function composite score for A05 sample; A05-LAN = language composite score for A05 sample.

participants were slightly older, less educated and included a higher proportion of men compared to CN Aβ- subjects in ADNI; no differences were detected in the A05. The symptomatic Aβ + groups showed the expected lower performance on neuropsychological tests in both studies.

3.1. Cognitive domain-specific tau-lesion networks

Fig. 2 shows the spatial overlap of the tau-PET lesions between the participants. The strongest overlap in tau-PET lesions was present in the medial temporal and posterior parietal brain regions (Fig. 2 A & B).

We employed lesion-network mapping and multivariate analysis in order to map functional connections of tau-PET lesions onto cognitive performance in each of the cognitive domains in our training sample (ADNI). For episodic memory performance, the associated tau-lesion network was primarily comprised of connections to the medial and lateral temporal cortex, angular gyrus, prefrontal cortex and precuneus/posterior cingulate cortex (Fig. 3A, column 1). The tau-lesion network of the executive-function domain was primarily comprised of tau-PET lesion connections to the pre- and post-central gyri, superior parietal cortex and lateral frontal cortex (Fig. 3B, column 1). Lastly, for the language domain, the network comprised primarily connections to the lateral temporal cortex, angular gyrus, prefrontal cortex, precuneus and cingulate cortex (Fig. 3C, column 1).

For each cognitive-domain specific network, results of linear regression analyses showed that stronger positive functional connectivity between the tau-lesion locations and the network regions was associated with lower performance in that cognitive domain in ADNI (Fig. 3 A-C, column 2) and in A05 (Fig. 3 A-C, column 3), suggesting that primarily those tau-PET lesions connected to the cognitive-domain specific network contributed to the worse performance in the respective cognitive domain.

Finally, in order to test for the specificity of the explanatory value of each network, we ran regression analyses for each pair of domain-specific network and a particular cognitive domain, controlling for the performance in the other cognitive domains. For ADNI, each domain-specific tau-lesion network predicted exclusively the performance in the matching but not the non-matching cognitive domains. An exception, however, was the language-domain tau-lesion network, where significance was lost to predict language performance, when controlling for memory and executive function performance (Supplementary Figure S1). For A05, the language-domain specific network showed a trend to predict language performance ($p = 0.058$), the executive function domain specifically predicted executive function, but the memory-domain network did not reach significance for the memory network when controlled for the other domains (Supplementary Figure S2), probably due to the fact that performance on the memory test and language tests are not entirely independent from each other.

3.2. Associations of subject-level functional connectivity alterations

First, we tested whether higher tau-PET W-scores are associated with altered functional connectivity within a cognitive-domain specific tau-lesion network in the Aβ + participants. Linear regression analysis showed that higher mean tau-PET W-scores in the tau lesion locations

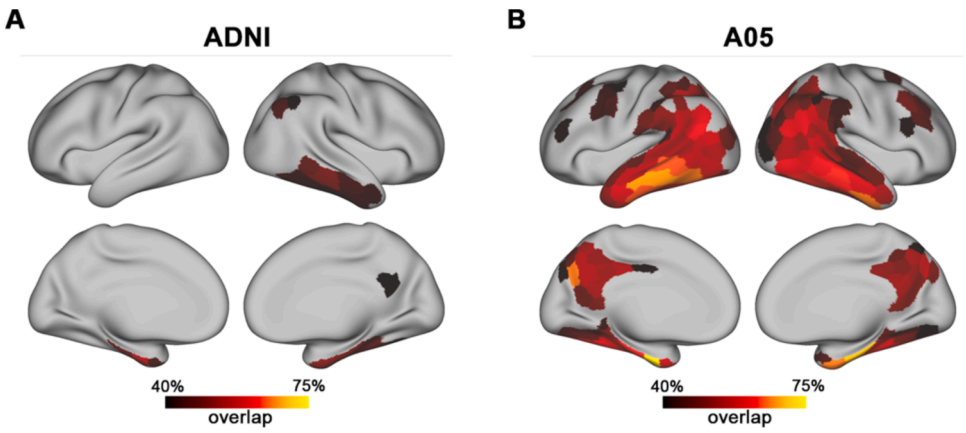

Fig. 2. Tau lesion and tau lesion network mapping in Alzheimer's disease. Brain surface renderings of the percentage of overlap in tau PET lesions (W-score > 2) across Aβ + patients in ADNI (A) and A05 (B), when thresholded at > 40 % overlap.

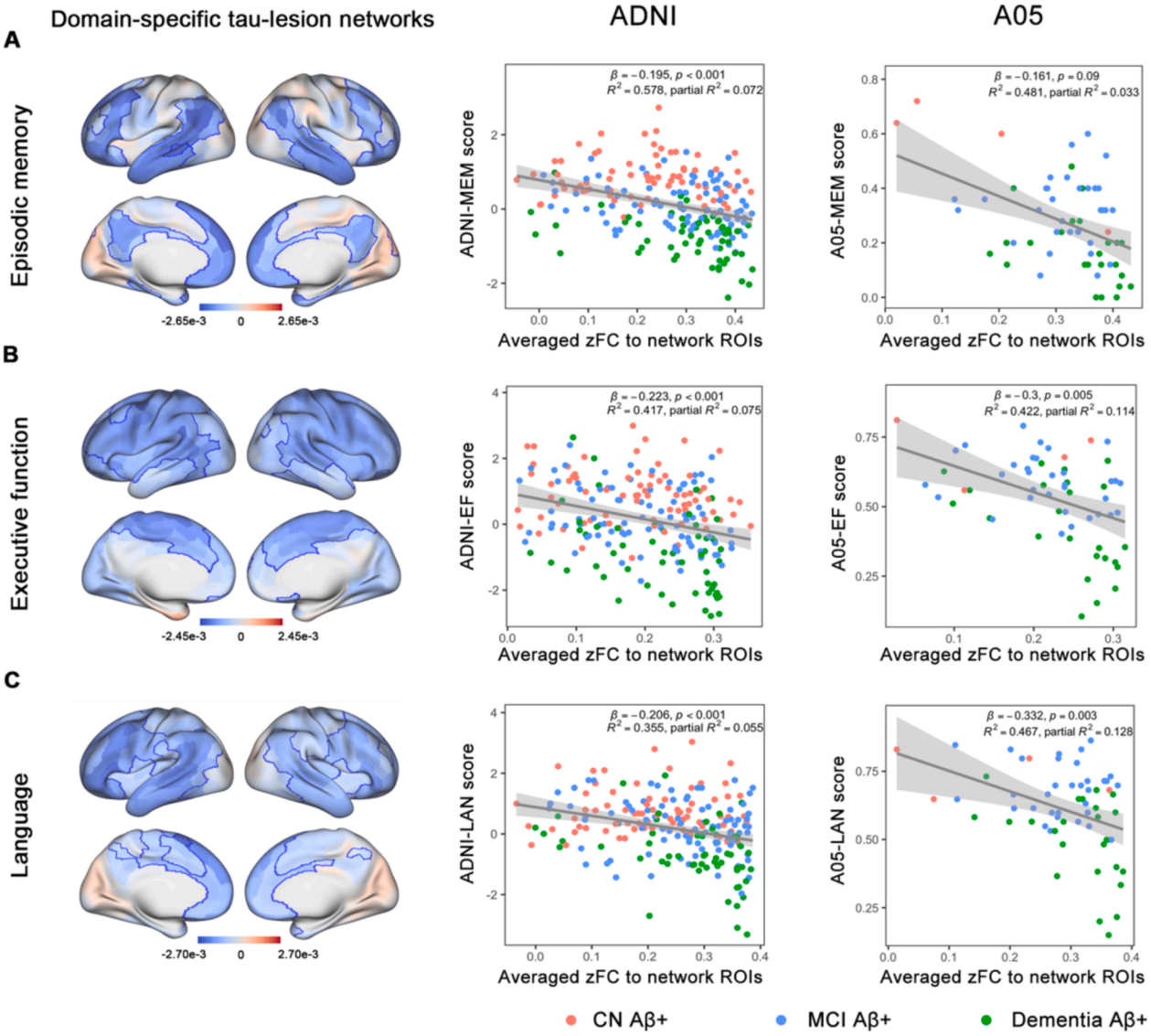

Fig. 3. Domain-specific tau-lesion network maps. The cognitive domain-specific tau-lesion networks derived from PLSR are rendered on the brain surface (1st column) for each cognitive domain in ADNI (rows A – C). Regression plots showing the association between the average of Fisher-z-transformed functional connectivity between tau lesion locations to each network and composite cognitive score for each cognitive domain (rows A – C) in ADNI (2nd column) and A05 (3nd column). The color-coding of the surface maps refers to the beta-coefficients of the association between connectivity and domain-specific cognitive performance. In the regression plots, the clinical classification of the subjects is color coded.

were associated with lower functional connectivity for each cognitive-domain specific tau-lesion network (Fig. 4). This finding suggests that higher tau accumulation is associated with disrupted connectivity to the domain-specific tau-lesion networks in Aβ + participants. In the analyses stratified by diagnostic group within the Aβ + participants, the associations also remained consistent in each diagnostic group (Supplementary Figures S3-5).

Next, we tested whether reduced functional connectivity in the domain-specific tau-lesion networks is associated with lower performance in the respective cognitive domain. In linear regression, we found that for each cognitive domain, weaker functional connectivity between tau lesions to the domain-specific tau-lesion network was associated with lower performance in the respective cognitive domain (Fig. 5). However, decreased functional connectivity to domain-specific tau-lesion network did not show significant mediation effect on the association between tau-PET W-scores and cognitive performances in corresponding cognitive domain.

4. Discussion

In the current study we investigated the brain's functional networks that are associated with tau-PET lesion locations in order to understand the interindividual variation in domain-specific cognitive impairment in AD. Firstly, locating subject-level tau-PET lesions within the normal functional connectome, we demonstrated that closer connectivity of tau-PET lesions to a domain-specific tau-lesion network is associated with stronger impairment in that cognitive domain. These cross-validated results suggest that it is the connectivity of brain location of tau-PET accumulation to the cognitive-domain specific tau-lesion networks which contribute to domain specific cognitive impairment. Secondly, we showed that higher tau-accumulation in a given brain location was associated with reduced connectivity to the associated domain-specific networks. Disrupted domain-specific-network connectivity was in turn associated with lower performance in the respective cognitive domain. Together, these findings suggest that functional connectivity of tau-PET locations provides an important link between regional tau-PET accumulation and the domain-specific cognitive impairment.

4.1. Tau-lesion network mapping explains phenotypic heterogeneity in AD

Our first finding mapping cognitive impairment onto tau-lesion networks is consistent with results from previous lesion network mapping studies which showed that the connectivity profile of local brain alterations is associated with psychiatric and cognitive symptoms (Boes et al., 2015; Darby et al., 2019; Fox, 2018; Tetreault et al., 2020). We advance these previous findings showing that it is the connectivity of the location of tau-PET accumulation to circumscribed cognitive domain specific networks that contributes to the explanation of region-dependent associations of tau with particular cognitive domains. This is an important finding given that the location of tau-PET deposition varies substantially between subjects (Fig. 2) (Franzmeier et al., 2020a; Vemuri et al., 2017). The connectivity pattern of spatially varying tau-PET lesion locations to a common domain-specific network provides a unifying scheme for leveraging the location of tau-PET accumulation for the explanation of domain-specific cognitive impairment. It is remarkable that the connectivity profile of a tau lesion alone is predictive of the severity of impairment in a particular cognitive domain, because the location alone is not indicative of the exact level of tau accumulation. Our findings demonstrate the utility of the lesion-network framework to link the locality of tau accumulation to cognitive decline in AD and to facilitate patient-level explanation of domain specific cognitive impairment. The discovered functional networks largely correspond to previous findings on mapping brain regions to cognitive domains including the temporo-parietal and frontal cortex for episodic memory (Tetreault et al., 2020; Amaefule et al., 2021; Ferguson et al., 2019; Huijbers et al., 2013; Kim, 2011; Simon-Vermot et al., 2018; Smith et al., 2009; Svaldi et al., 2021), and fronto-parietal regions for executive function (Cole et al., 2014; Cole and Schneider, 2007). We note, however, that our results do not imply that all brain regions of a domain-specific network are essential for the cognitive domain. Rather, the contribution of a particular brain region to performance in a cognitive domain is proportional to its connectivity to a domain-specific tau-lesion network. Furthermore, our results suggest that the domain-specific tau-lesion networks show a preponderance of explanatory power for the matching cognitive domain, but the nature of domain-specificity is one that varies by degree rather than in an all-or-none fashion.

4.2. Connectivity alterations in the tau-PET lesion network

Having determined the spatial signature of the cognitive domain-specific tau-lesion networks we next showed that the functional connectivity alterations in the cognitive domain-specific tau-lesion networks were associated with cognitive decline. Specifically, we found that weaker connectivity of a tau-lesion's network was associated with lower cognitive performance. These findings are consistent with previous results showing that higher biomarker levels of tau pathology in the

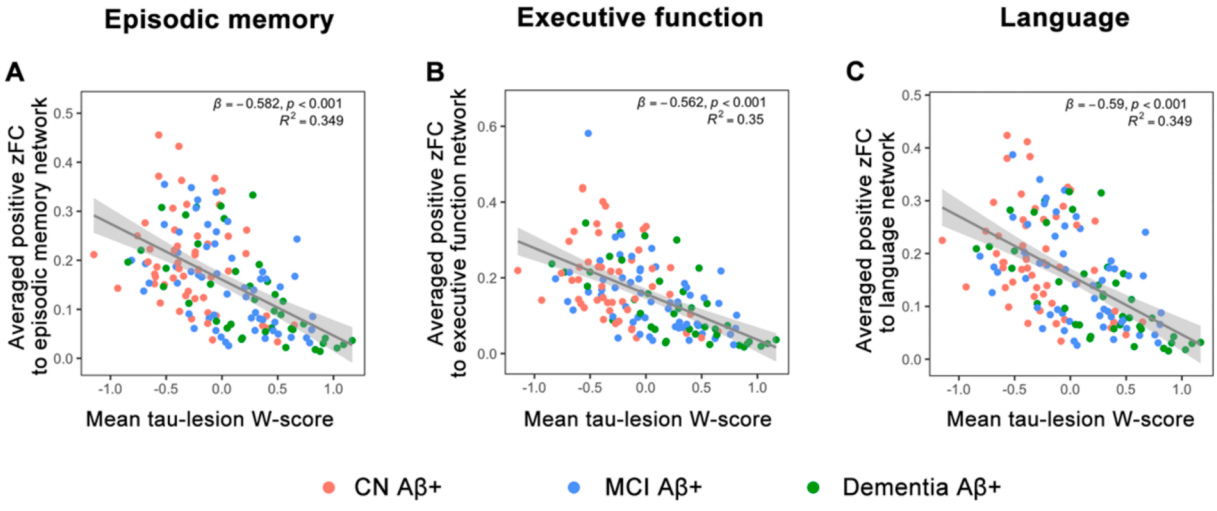

Fig. 4. Association between tau-PET and patient-level domain-specific network connectivity. For each cognitive domain (A-C), the scatterplots show the associations between tau-PET W-scores averaged across tau lesions and domain-specific tau-lesion networks connectivity (Fisher Z-transformed). The diagnostic classification is color labeled.

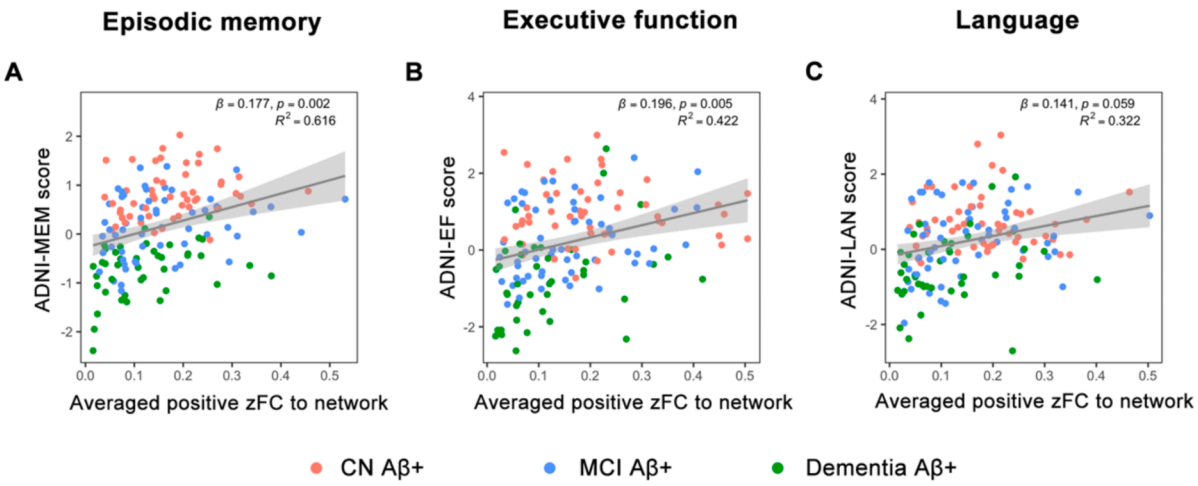

Fig. 5. Association between patient-level domain-specific network connectivity and cognitive decline. For each domain-specific tau-lesion network (A-C), the scatterplots show the association between the average functional connectivity of tau-PET lesions to domain-specific tau-lesion network ROIs (Fisher Z-transformed) and the performance in each cognitive domain. The diagnostic classification is color labeled.

presence of Aβ are associated with lower functional connectivity and lower brain activity (Berron et al., 2021; Pereira et al., 2019; Schultz et al., 2017), supporting the view that functional connectivity changes are a crucial endophenotype linking tau pathology and cognitive decline. Our results provide mechanistic insight into why the locality of tau-PET lesions matter for explaining decline in specific cognitive domains, supporting the view that disrupted connectivity in domain-specific tau-lesion network underlie the effects of regional tau-PET on specific cognitive abilities. The exact mechanism by which tau pathology may disrupt have not been deciphered yet. However, tau has been associated with neuronal silencing in mouse models of amyloid and tau pathology (Busche et al., 2019), which may contribute to the disruption of functional connectivity. Furthermore, in vitro and in vivo preclinical research showed that pathologic tau is transmitted along axons and spread in a prion-like manner (Clavaguera et al., 2009; Kaufman et al., 2017), therefore the development of pathologic tau is intrinsically linked to the architecture of the brain's connectome. In patients with AD, we and others previously showed that tau-PET accumulation is distributed particularly between strongly connected brain regions (Franzmeier et al., 2020b; Franzmeier et al., 2019; Vogel et al., 2023; Vogel et al., 2021), consistent with the notion that pathologic tau preferentially spreads along axonal connections. Importantly, axonal connections may not only serve as conduits for pathological tau, but are also the target of tau-related impairment, where higher tau pathology is associated with reduced axonal and myelin integrity of fiber tracts (Dean et al., 2017; Pichet Binette et al., 2021). Therefore, tau-related fiber-tract damage is a putative pathway leading to functional disconnection. Conversely, enhancing functional and structural networks are therefore putative targets for therapeutic intervention to enhance the cognitive resilience against the effect of tau pathology (Ewers et al., 2021; Neitzel et al., 2019).

In order to interpret the current findings, several caveats should be considered. First, our lesion-symptom mapping approach employed a fMRI template from the Human Connectome Project that included young to middle-aged adults, whereas our patient samples comprised exclusively elderly subjects with AD pathology. The alternate application of connectome maps from elderly cognitively normal subjects may have enhanced the accuracy to map the connectome to tau-PET lesions. However, the disadvantage of that approach is that in cognitively normal elderly some critical connections may have been already lost due to age or incipient disease. Note that our analysis of functional connectivity assessed in the patients confirmed an effect of tau-PET on the connectivity in the identified cognitive domain specific tau-lesion networks, supporting that we detected core networks underlying domain-specific cognitive performance. Second, the current study is cross-sectional in nature, and the utility to predict longitudinal changes remains to be tested. Third, the current samples mostly included Caucasian subjects, where other ethnicities were underrepresented. Dedicated research efforts are underway to alleviate the recruitment bias in observational and clinical trials. Thus, the generalizability across different ethnic group remains unclear so far.

Overall, the major contribution of the current study is the demonstration of the utility of domain-specific connectivity patterns of tau-PET lesion locations that can be leveraged to explain domain-specific cognitive impairment. We provide an approach to understand symptomatic heterogeneity in AD, which may help to reduce uncertainty in the clinical diagnosis of AD.

Data availability.

Data of ADNI used in this study are available from the ADNI website (www.adni-info.org). Resting-state fMRI data of HCP are available online (https://db.humanconnectome.org). Data of A05 are available upon request to the 18F-AV1451-A05 investigators.

CRediT authorship contribution statement

Ying Luan: Writing – review & editing, Writing – original draft, Visualization, Validation, Formal analysis. **Anna Rubinski:** Writing – review & editing. **Davina Biel:** Writing – review & editing. **Diana Otero Svaldi:** Writing – review & editing, Data curation. **Ixavier Alonzo Higgins:** Writing – review & editing, Data curation. **Sergey Shcherbinin:** Writing – review & editing, Data curation. **Michael Pontecorvo:** Writing – review & editing, Writing – original draft, Supervision, Project administration, Funding acquisition, Conceptualization. **Nicolai Franzmeier:** Writing – review & editing, Conceptualization. **Michael Ewers:** Writing – review & editing, Writing – original draft, Supervision, Project administration, Funding acquisition, Conceptualization.

Funding

The study was supported by the German Center for Neurodegenerative Diseases (DZNE), the Deutsche Forschungsgemeinschaft (DFG, German Research Foundation) grant for major research instrumentation (DFG, INST 409/193–1 FUGG) and the Legerlotz Stiftung (to ME).

ADNI data collection and sharing for this project was funded by the ADNI (National Institutes of Health Grant U01 AG024904) and DOD ADNI (Department of Defense award number W81XWH-12–2-0012). ADNI is funded by the National Institute on Aging, the National Institute of Biomedical Imaging, and Bioengineering, and through contributions

from the following: AbbVie, Alzheimer's Association; Alzheimer's Drug Discovery Foundation; Araclon Biotech; BioClinica, Inc.; Biogen; Bristol-Myers Squibb Company; CereSpir, Inc.; Cogstate; Eisai Inc.; Elan Pharmaceuticals, Inc.; Eli Lilly and Company; EuroImmun; F. Hoffmann-La Roche Ltd and its affiliated company Genentech, Inc.; Fujirebio; GE Healthcare; IXICO Ltd.; Janssen Alzheimer Immunotherapy Research & Development, LLC.; Johnson & Johnson Pharmaceutical Research & Development LLC.; Lumosity; Lundbeck; Merck & Co., Inc.; Meso Scale Diagnostics, LLC.; NeuroRx Research; Neurotrack Technologies; Novartis Pharmaceuticals Corporation; Pfizer Inc.; Piramal Imaging; Servier; Takeda Pharmaceutical Company; and Transition Therapeutics. The Canadian Institutes of Health Research is providing funds to support ADNI clinical sites in Canada. Private sector contributions are facilitated by the Foundation for the National Institutes of Health (https://www.fnih.org).

Declaration of Competing Interest

The authors declare that they have no known competing financial interests or personal relationships that could have appeared to influence the work reported in this paper.

Acknowledgment

Parts of the data used in preparation of this manuscript were obtained from the ADNI database (adni.loni.usc.edu). As such, the investigators within the ADNI study contributed to the design and implementation of ADNI and/or provided data but did not participate in analysis or writing of this paper. A complete listing of ADNI investigators can be found in the Appendix.

Appendix A. Supplementary data

Supplementary data to this article can be found online at https://doi.org/10.1016/j.nicl.2024.103699.

Data availability

Data will be made available on request.

References

Alzheimer's Association, 2020. 2020 Alzheimer's disease facts and figures. Alzheimers Dement Online ahead of print.

Amaefule, C.O., Dyrba, M., Wolfsgruber, S., Polcher, A., Schneider, A., Fliessbach, K., Spottke, A., Meiberth, D., Preis, L., Peters, O., Incesoy, E.I., Spruth, E.J., Priller, J., Altenstein, S., Bartels, C., Wiltfang, J., Janowitz, D., Burger, K., Laske, C., Munk, M., Rudolph, J., Glanz, W., Dobisch, L., Haynes, J.D., Dechent, P., Ertl-Wagner, B., Scheffler, K., Kilimann, I., Duzel, E., Metzger, C.D., Wagner, M., Jessen, F., Teipel, S. J., 2021. Association between composite scores of domain-specific cognitive functions and regional patterns of atrophy and functional connectivity in the Alzheimer's disease spectrum. Neuroimage. Clin. 29, 102533.

Avants, B.B., Tustison, N.J., Song, G., Cook, P.A., Klein, A., Gee, J.C., 2011. A reproducible evaluation of ANTs similarity metric performance in brain image registration. Neuroimage 54, 2033–2044.

Beckmann, C.F., Smith, S.M., 2004. Probabilistic independent component analysis for functional magnetic resonance imaging. IEEE Trans. Med. Imaging 23, 137–152.

Bejanin, A., Schonhaut, D.R., La Joie, R., Kramer, J.H., Baker, S.L., Sosa, N., Ayakta, N., Cantwell, A., Janabi, M., Lauriola, M., O'Neil, J.P., Gorno-Tempini, M.L., Miller, Z. A., Rosen, H.J., Miller, B.L., Jagust, W.J., Rabinovici, G.D., 2017. Tau pathology and neurodegeneration contribute to cognitive impairment in Alzheimer's disease. Brain 140, 3286–3300.

Berron, D., Vogel, J.W., Insel, P.S., Pereira, J.B., Xie, L., Wisse, L.E.M., Yushkevich, P.A., Palmqvist, S., Mattsson-Carlgren, N., Stomrud, E., Smith, R., Strandberg, O., Hansson, O., 2021. Early stages of tau pathology and its associations with functional connectivity, atrophy and memory. Brain.

Boes, A.D., Prasad, S., Liu, H., Liu, Q., Pascual-Leone, A., Caviness Jr., V.S., Fox, M.D., 2015. Network localization of neurological symptoms from focal brain lesions. Brain 138, 3061–3075.

Braak, H., Braak, E., 1991. Neuropathological stageing of Alzheimer-related changes. Acta Neuropathol. 82, 239–259.

Braak, H., Del Tredici, K., 2018. Spreading of Tau Pathology in Sporadic Alzheimer's Disease Along Cortico-cortical Top-Down Connections. Cereb. Cortex 28, 3372–3384.

Busche, M.A., Wegmann, S., Dujardin, S., Commins, C., Schiantarelli, J., Klickstein, N., Kamath, T.V., Carlson, G.A., Nelken, I., Hyman, B.T., 2019. Tau impairs neural circuits, dominating amyloid-beta effects, in Alzheimer models in vivo. Nat. Neurosci. 22, 57–64.

Clavaguera, F., Bolmont, T., Crowther, R.A., Abramowski, D., Frank, S., Probst, A., Fraser, G., Stalder, A.K., Beibel, M., Staufenbiel, M., Jucker, M., Goedert, M., Tolnay, M., 2009. Transmission and spreading of tauopathy in transgenic mouse brain. Nat. Cell Biol. 11, 909–913.

Cole, M.W., Repovs, G., Anticevic, A., 2014. The frontoparietal control system: a central role in mental health. Neuroscientist 20, 652–664.

Cole, M.W., Schneider, W., 2007. The cognitive control network: Integrated cortical regions with dissociable functions. Neuroimage 37, 343–360.

Darby, R.R., Laganiere, S., Pascual-Leone, A., Prasad, S., Fox, M.D., 2017. Finding the imposter: brain connectivity of lesions causing delusional misidentifications. Brain 140, 497–507.

Darby, R.R., Joutsa, J., Fox, M.D., 2019. Network localization of heterogeneous neuroimaging findings. Brain 142, 70–79.

Dean 3rd, D.C., Hurley, S.A., Kecskemeti, S.R., O'Grady, J.P., Canda, C., Davenport-Sis, N.J., Carlsson, C.M., Zetterberg, H., Blennow, K., Asthana, S., Sager, M.A., Johnson, S.C., Alexander, A.L., Bendlin, B.B., 2017. Association of Amyloid Pathology With Myelin Alteration in Preclinical Alzheimer Disease. JAMA Neurol. 74, 41–49.

Devous Sr., M.D., Fleisher, A.S., Pontecorvo, M.J., Lu, M., Siderowf, A., Navitsky, M., Kennedy, I., Southekal, S., Harris, T.S., Mintun, M.A., 2021. Relationships Between Cognition and Neuropathological Tau in Alzheimer's Disease Assessed by 18F Flortaucipir PET. J. Alzheimers Dis. 80, 1091–1104.

Digma, L.A., Madsen, J.R., Reas, E.T., Dale, A.M., Brewer, J.B., Banks, S.J., Alzheimer's Disease Neuroimaging, I., 2019. Tau and atrophy: domain-specific relationships with cognition. Alzheimers Res. Ther. 11, 65.

Ewers, M., Luan, Y., Frontzkowski, L., Neitzel, J., Rubinski, A., Dichgans, M., Hassenstab, J., Gordon, B.A., Chhatwal, J.P., Levin, J., Schofield, P., Benzinger, T.L.S., Morris, J. C., Goate, A., Karch, C.M., Fagan, A.M., McDade, E., Allegri, R., Berman, S., Chui, H., Cruchaga, C., Farlow, M., Graff-Radford, N., Jucker, M., Lee, J.H., Martins, R.N., Mori, H., Perrin, R., Xiong, C., Rossor, M., Fox, N.C., O'Connor, A., Salloway, S., Danek, A., Buerger, K., Bateman, R.J., Habeck, C., Stern, Y., Franzmeier, N., Alzheimer's Disease Neuroimaging, I., the Dominantly Inherited Alzheimer, N., 2021. Segregation of functional networks is associated with cognitive resilience in Alzheimer's disease. Brain 144, 2176-2185.

Ferguson, M.A., Lim, C., Cooke, D., Darby, R.R., Wu, O., Rost, N.S., Corbetta, M., Grafman, J., Fox, M.D., 2019. A human memory circuit derived from brain lesions causing amnesia. Nat. Commun. 10, 3497.

Fox, M.D., 2018. Mapping Symptoms to Brain Networks with the Human Connectome. N. Engl. J. Med. 379, 2237–2245.

Franzmeier, N., Rubinski, A., Neitzel, J., Kim, Y., Damm, A., Na, D.L., Kim, H.J., Lyoo, C. H., Cho, H., Finsterwalder, S., Duering, M., Seo, S.W., Ewers, M., 2019. Functional connectivity associated with tau levels in ageing, Alzheimer's, and small vessel disease. Brain 142, 1093–1107.

Franzmeier, N., Dewenter, A., Frontzkowski, L., Dichgans, M., Rubinski, A., Neitzel, J., Smith, R., Strandberg, O., Ossenkoppele, R., Buerger, K., Duering, M., Hansson, O., Ewers, M., 2020a. Patient-centered connectivity-based prediction of tau pathology spread in Alzheimer's disease. Sci. Adv. 6.

Franzmeier, N., Neitzel, J., Rubinski, A., Smith, R., Strandberg, O., Ossenkoppele, R., Hansson, O., Ewers, M., Alzheimer's Disease Neuroimaging, I., 2020b. Functional brain architecture is associated with the rate of tau accumulation in Alzheimer's disease. Nat. Commun. 11, 347.

Huijbers, W., Schultz, A.P., Vannini, P., McLaren, D.G., Wigman, S.E., Ward, A.M., Hedden, T., Sperling, R.A., 2013. The encoding/retrieval flip: interactions between memory performance and memory stage and relationship to intrinsic cortical networks. J. Cogn. Neurosci. 25, 1163–1179.

Jagust, W.J., Landau, S.M., Koeppe, R.A., Reiman, E.M., Chen, K., Mathis, C.A., Price, J. C., Foster, N.L., Wang, A.Y., 2015. The Alzheimer's Disease Neuroimaging Initiative 2 PET Core: 2015. Alzheimers Dement. 11, 757–771.

Kaufman, S.K., Thomas, T.L., Del Tredici, K., Braak, H., Diamond, M.I., 2017. Characterization of tau prion seeding activity and strains from formaldehyde-fixed tissue. Acta Neuropathol. Commun. 5, 41.

Kim, H., 2011. Neural activity that predicts subsequent memory and forgetting: a meta-analysis of 74 fMRI studies. Neuroimage 54, 2446–2461.

Krishnan, A., Williams, L.J., McIntosh, A.R., Abdi, H., 2011. Partial Least Squares (PLS) methods for neuroimaging: a tutorial and review. Neuroimage 56, 455–475.

La Joie, R., Visani, A.V., Baker, S.L., Brown, J.A., Bourakova, V., Cha, J., Chaudhary, K., Edwards, L., Iaccarino, L., Janabi, M., Lesman-Segev, O.H., Miller, Z.A., Perry, D.C., O'Neil, J.P., Pham, J., Rojas, J.C., Rosen, H.J., Seeley, W.W., Tsai, R.M., Miller, B.L., Jagust, W.J., Rabinovici, G.D., 2020. Prospective longitudinal atrophy in Alzheimer's disease correlates with the intensity and topography of baseline tau-PET. Sci. Transl. Med. 12, eaau5732.

Langbaum, J.B., Hendrix, S.B., Ayutyanont, N., Chen, K., Fleisher, A.S., Shah, R.C., Barnes, L.L., Bennett, D.A., Tariot, P.N., Reiman, E.M., 2014. An empirically derived composite cognitive test score with improved power to track and evaluate treatments for preclinical Alzheimer's disease. Alzheimers Dement. 10, 666–674.

Malek-Ahmadi, M., Chen, K., Perez, S.E., He, A., Mufson, E.J., 2018. Cognitive composite score association with Alzheimer's disease plaque and tangle pathology. Alzheimers Res. Ther. 10, 90.

Miller, K.L., Alfaro-Almagro, F., Bangerter, N.K., Thomas, D.L., Yacoub, E., Xu, J., Bartsch, A.J., Jbabdi, S., Sotiropoulos, S.N., Andersson, J.L., Griffanti, L., Douaud, G., Okell, T.W., Weale, P., Dragonu, I., Garratt, S., Hudson, S., Collins, R., Jenkinson, M., Matthews, P.M., Smith, S.M., 2016. Multimodal population brain imaging in the UK Biobank prospective epidemiological study. Nat. Neurosci. 19, 1523–1536.

Mohanty, R., Ferreira, D., Nordberg, A., Westman, E., Alzheimer's Disease Neuroimaging, I., 2023. Associations between different tau-PET patterns and longitudinal atrophy in the Alzheimer's disease continuum: biological and methodological perspectives from disease heterogeneity. Alzheimers Res. Ther. 15, 37.

Murray, M.E., Graff-Radford, N.R., Ross, O.A., Petersen, R.C., Duara, R., Dickson, D.W., 2011. Neuropathologically defined subtypes of Alzheimer's disease with distinct clinical characteristics: a retrospective study. Lancet Neurol. 10, 785–796.

Neitzel, J., Franzmeier, N., Rubinski, A., Ewers, M., Alzheimer's Disease Neuroimaging, I., 2019. Left frontal connectivity attenuates the adverse effect of entorhinal tau pathology on memory. Neurology 93, e347–e357.

Nelson, P.T., Alafuzoff, I., Bigio, E.H., Bouras, C., Braak, H., Cairns, N.J., Castellani, R.J., Crain, B.J., Davies, P., Del Tredici, K., Duyckaerts, C., Frosch, M.P., Haroutunian, V., Hof, P.R., Hulette, C.M., Hyman, B.T., Iwatsubo, T., Jellinger, K.A., Jicha, G.A., Kovari, E., Kukull, W.A., Leverenz, J.B., Love, S., Mackenzie, I.R., Mann, D.M., Masliah, E., McKee, A.C., Montine, T.J., Morris, J.C., Schneider, J.A., Sonnen, J.A., Thal, D.R., Trojanowski, J.Q., Troncoso, J.C., Wisniewski, T., Woltjer, R.L., Beach, T. G., 2012. Correlation of Alzheimer disease neuropathologic changes with cognitive status: a review of the literature. J. Neuropathol. Exp. Neurol. 71, 362–381.

Ossenkoppele, R., Cohn-Sheehy, B.I., La Joie, R., Vogel, J.W., Moller, C., Lehmann, M., van Berckel, B.N., Seeley, W.W., Pijnenburg, Y.A., Gorno-Tempini, M.L., Kramer, J. H., Barkhof, F., Rosen, H.J., van der Flier, W.M., Jagust, W.J., Miller, B.L., Scheltens, P., Rabinovici, G.D., 2015. Atrophy patterns in early clinical stages across distinct phenotypes of Alzheimer's disease. Hum. Brain Mapp. 36, 4421–4437.

Pereira, J.B., Ossenkoppele, R., Palmqvist, S., Strandberg, T.O., Smith, R., Westman, E., Hansson, O., 2019. Amyloid and tau accumulate across distinct spatial networks and are differentially associated with brain connectivity. Elife 8.

Petersen, R.C., Aisen, P.S., Beckett, L.A., Donohue, M.C., Gamst, A.C., Harvey, D.J., Jack Jr., C.R., Jagust, W.J., Shaw, L.M., Toga, A.W., Trojanowski, J.Q., Weiner, M. W., 2010. Alzheimer's Disease Neuroimaging Initiative (ADNI): clinical characterization. Neurology 74, 201–209.

Pichet Binette, A., Theaud, G., Rheault, F., Roy, M., Collins, D.L., Levin, J., Mori, H., Lee, J.H., Farlow, M.R., Schofield, P., Chhatwal, J.P., Masters, C.L., Benzinger, T., Morris, J., Bateman, R., Breitner, J.C., Poirier, J., Gonneaud, J., Descoteaux, M., Villeneuve, S., Group, D.S., Group, P.-A.R., 2021. Bundle-specific associations between white matter microstructure and Abeta and tau pathology in preclinical Alzheimer's disease. Elife 10.

Pontecorvo, M.J., Devous Sr., M.D., Navitsky, M., Lu, M., Salloway, S., Schaerf, F.W., Jennings, D., Arora, A.K., McGeehan, A., Lim, N.C., Xiong, H., Joshi, A.D., Siderowf, A., Mintun, M.A., Investigators, F.A.-A., 2017. Relationships between flortaucipir PET tau binding and amyloid burden, clinical diagnosis, age and cognition. Brain 140, 748–763.

Pontecorvo, M.J., Devous, M.D., Kennedy, I., Navitsky, M., Lu, M., Galante, N., Salloway, S., Doraiswamy, P.M., Southekal, S., Arora, A.K., McGeehan, A., Lim, N.C., Xiong, H., Truocchio, S.P., Joshi, A.D., Shcherbinin, S., Teske, B., Fleisher, A.S., Mintun, M.A., 2019. A multicentre longitudinal study of flortaucipir (18F) in normal ageing, mild cognitive impairment and Alzheimer's disease dementia. Brain 142, 1723–1735.

Schaefer, A., Kong, R., Gordon, E.M., Laumann, T.O., Zuo, X.N., Holmes, A.J., Eickhoff, S. B., Yeo, B.T.T., 2018. Local-Global Parcellation of the Human Cerebral Cortex from Intrinsic Functional Connectivity MRI. Cereb. Cortex 28, 3095–3114.

Schultz, A.P., Chhatwal, J.P., Hedden, T., Mormino, E.C., Hanseeuw, B.J., Sepulcre, J., Huijbers, W., LaPoint, M., Buckley, R.F., Johnson, K.A., Sperling, R.A., 2017. Phases of Hyperconnectivity and Hypoconnectivity in the Default Mode and Salience Networks Track with Amyloid and Tau in Clinically Normal Individuals. J. Neurosci. 37, 4323–4331.

Simon-Vermot, L., Taylor, A.N.W., Araque Caballero, M.A., Franzmeier, N., Buerger, K., Catak, C., Janowitz, D., Kambeitz-Ilankovic, L.M., Ertl-Wagner, B., Duering, M., Ewers, M., 2018. Correspondence Between Resting-State and Episodic Memory-Task Related Networks in Elderly Subjects. Front. Aging Neurosci. 10, 362.

Smith, S.M., Fox, P.T., Miller, K.L., Glahn, D.C., Fox, P.M., Mackay, C.E., Filippini, N., Watkins, K.E., Toro, R., Laird, A.R., Beckmann, C.F., 2009. Correspondence of the brain's functional architecture during activation and rest. PNAS 106, 13040–13045.

Smith, S.M., Beckmann, C.F., Andersson, J., Auerbach, E.J., Bijsterbosch, J., Douaud, G., Duff, E., Feinberg, D.A., Griffanti, L., Harms, M.P., Kelly, M., Laumann, T., Miller, K. L., Moeller, S., Petersen, S., Power, J., Salimi-Khorshidi, G., Snyder, A.Z., Vu, A.T., Woolrich, M.W., Xu, J., Yacoub, E., Ugurbil, K., Van Essen, D.C., Glasser, M.F., Consortium, W.U.-M.H., 2013. Resting-state fMRI in the Human Connectome Project. Neuroimage 80, 144-168.

Svaldi, D.O., Goni, J., Abbas, K., Amico, E., Clark, D.G., Muralidharan, C., Dzemidzic, M., West, J.D., Risacher, S.L., Saykin, A.J., Apostolova, L.G., 2021. Optimizing differential identifiability improves connectome predictive modeling of cognitive deficits from functional connectivity in Alzheimer's disease. Hum. Brain Mapp. 42, 3500–3516.

Tetreault, A.M., Phan, T., Orlando, D., Lyu, I., Kang, H., Landman, B., Darby, R.R., Neuroimaging, A.D., I.,, 2020. Network localization of clinical, cognitive, and neuropsychiatric symptoms in Alzheimer's disease. Brain 143, 1249–1260.

Vemuri, P., Lowe, V.J., Knopman, D.S., Senjem, M.L., Kemp, B.J., Schwarz, C.G., Przybelski, S.A., Machulda, M.M., Petersen, R.C., Jack Jr., C.R., 2017. Tau-PET uptake: Regional variation in average SUVR and impact of amyloid deposition. Alzheimers Dement (amst) 6, 21–30.

Vogel, J.W., Young, A.L., Oxtoby, N.P., Smith, R., Ossenkoppele, R., Strandberg, O.T., La Joie, R., Aksman, L.M., Grothe, M.J., Iturria-Medina, Y., Pontecorvo, M.J., Devous, M.D., Rabinovici, G.D., Alexander, D.C., Lyoo, C.H., Evans, A.C., Hansson, O., 2021. Four distinct trajectories of tau deposition identified in Alzheimer's disease. Nat. Med. 27, 871–881.

Vogel, J.W., Corriveau-Lecavalier, N., Franzmeier, N., Pereira, J.B., Brown, J.A., Maass, A., Botha, H., Seeley, W.W., Bassett, D.S., Jones, D.T., Ewers, M., 2023. Connectome-based modelling of neurodegenerative diseases: towards precision medicine and mechanistic insight. Nat. Rev. Neurosci. 24, 620–639.

Weiner, M.W., Veitch, D.P., Aisen, P.S., Beckett, L.A., Cairns, N.J., Green, R.C., Harvey, D., Jack Jr., C.R., Jagust, W., Morris, J.C., Petersen, R.C., Salazar, J., Saykin, A.J., Shaw, L.M., Toga, A.W., Trojanowski, J.Q., Neuroimaging, A.D., I.,, 2017. The Alzheimer's Disease Neuroimaging Initiative 3: Continued innovation for clinical trial improvement. Alzheimers Dement. 13, 561–571.